Journal of New Technology and Materials (JNTM)
J. New Technol. Mater.
Vol. 12, N°01 (2022)55-62

OEB Univ. Publish. Co.

Physical properties of nanostructured TiO_2 thin films grown by RF magnetron sputtering: Impact of substrate type

S. Khodja[a], T. Touam[b*] and A. Chelouche[c]

[a]*Radiation and Plasma and Surface Physics Laboratory, University Kasdi Merbah Ouargla, Ouargla 30000, Algeria*

[b]*Semiconductors Laboratory, University Badji Mokhtar-Annaba, Annaba 23000, Algeria*

[c]*Laboratory of Environmental Engineering, University of Bejaia, Bejaia 06000, Algeria*

*Corresponding author, email: touamt@gmail.com

Received date: March 6, 2022 ; accepted date: May 22, 2022

Abstract

Titanium dioxide (TiO_2) thin films were successfully prepared on three different substrates (glass, quartz and silicon (Si(100)) at room temperature with a deposition time of 90 min using RF magnetron sputtering technique. The TiO_2 thin films are then air-annealed at 400°C for one hour and the effect of the substrate type on the microstructure, morphology, surface topography, transmittance and optical band gap of these films was investigated by X-ray diffraction (XRD), Raman spectroscopy, scanning electron microscopy (SEM), atomic force microscopy (AFM) and UV-Visible (UV-Vis) spectrophotometry. XRD analysis showed that all thin films are polycrystalline and crystallize only in the tetragonal anatase structure of TiO_2 with a preferential orientation along the (101) plane. The crystallinity, peak intensity, and crystallite growth are found to be substrate type dependent. The observed Raman peaks confirmed the presence of anatase phase in all samples in good agreement with XRD data. SEM and AFM images revealed that TiO_2 thin films exhibit a different surface topography, which seems to be influenced by the substrate type, as expressed in terms of average grain size and surface roughness. Transmittance spectra put into evidence that the TiO_2 thin film grown on quartz demonstrated a higher average transmission in the visible region than that deposited on glass substrate. Moreover, the obtained values of band gap and refractive index for TiO_2 thin films deposited on glass and quartz substrates were found to be 3.615 and 3.512 eV, and 2.248 and 2.271, respectively.

Keywords: TiO_2 thin films; RF sputtering; Substrate type; microstructural study; optical properties; optoelectronic applications

1. Introduction

During the recent years, titanium dioxide (TiO_2) has been the most extensively investigated material. This great enthusiasm is due to its outstanding properties such as long durability, non-toxic nature, availability, robustness [1–3], gas sensors [4], photocatalysts [5], multilayer optical coatings [6] and optical wave guides [7]. Moreover, according to electrochemical properties, TiO_2 is known to be an n-type semiconductor [8]. All TiO_2 polymorphs are low-cost semiconductor materials with high transparency, wide optical bandgap range (3.0–3.2 eV) [9–11], biocompatibility and high chemical stability [12]. Since TiO_2 is characterized by a high chemical stability and a modest band gap it is suitable for fabricating dye-sensitized solar cells [13]. With a high refractive index TiO_2 transmits visible light (600–800 nm) but absorbs UV light (200–300 nm) [14]. On the other hand, it is well established that TiO_2 exists in three different crystalline structures; anatase (trigonal), rutile (tetragonal) and brookite (orthorhombic) [15]. Therefore, Rutile is the stable high temperature phase (generally in the 600–1855°C), whereas anatase and brookite are metastable and are readily transformed to rutile when heated [16].

Many techniques have been used to deposit TiO_2 thin films such as e-beam evaporation [17], chemical vapor deposition [18], sol-gel process [19], spray pyrolysis [20], hydrothermal method [21], metal–organic chemical vapor deposition [22], pulsed laser deposition [23], the ion beam technique,[24], plasma enhanced chemical vapor deposition (PECVD)[25], electrophoretic [26], screen printing [27] and radio frequency (RF) magnetron sputtering [28–30]. Among these methods, magnetron sputtering which is an industrial process applicable to large-area deposition [31] has many advantageous characteristics such as lower substrate temperature, good film adhesion, good uniformity of thickness distribution, the film properties can be easily modified by doping.

Thus, the RF Magnetron sputtering method has the ability to produce good quality thin films. However, there are many parameters which could influence the properties of RF sputtered thin films such as sputtering power [32], growing temperature [33], sputtering time [34], sputtering pressure [35], partial pressure [36], substrate-to-target distance [37]. However, substrate type is one of the most

interesting parameters in the preparation of TiO_2 nanostructured thin films. It has also been shown that by increasing growth temperature with different substrates [2], the structural properties of TiO_2 thin films can be modified, and consequently its optical constants and absorption spectra.

Several researches on RF Magnetron Sputtering TiO_2 thin film physical properties have been reported with different deposition parameters [38–42]. However a few works have discussed the effect of substrate type on thin films properties. It has been reported that that materials such as glass and quartz are widely used as substrates due to their high transmittance [43–45]. In addition Meng *et al.* [46] and Nair *et al.* [47] have also used a quartz substrate to prevent light refraction. Sun *et al.* [48] reported that TiO_2 coated on glass has good antibacterial, disinfectant, antifogging, and self-cleaning properties.

In this work, TiO_2 thin films were first grown on glass, quartz and Si(100) substrates at room temperature with a deposition time of 60 min using RF magnetron sputtering technique. Then, all samples were annealed during 1 hour at 400°C and the influence of substrate type on the microstructure, morphology, surface topography and optical properties of the TiO_2 thin films was investigated by by using various characterization techniques.

2. Experimental

2.1. Thin film preparation

TiO_2 thin films were deposited by RF magnetron sputtering on glass, quartz and Si(100) substrates at room temperature from a 2-inch diameter commercial TiO_2 ceramic target with 99.99% purity. Prior to deposition, all substrates were degreased by detergent and rinsed with distilled water, ultrasonically cleaned using acetone, methanol, and deionized water, and then dried in blowing nitrogen. The sputtering chamber was initially evacuated to a base pressure of 3×10^{-6} mbar before the introduction of pure argon gas at a flow rate of 30 sccm (standard cubic centimeters per minute). During deposition, working pressure was fixed at 2×10^{-3} mbar using a VAT valve controller. An RF power of 200 W was applied to the TiO_2 target. The operating distance between the substrate and the target was kept at 150 mm. A presputtering for about 25 min was done to remove contaminants from the surface of the target and to stabilize the sputtering process. The TiO_2 thin films were grown for a deposition time of 90 minutes. After that, a post-deposition annealing step was performed at 400°C for 1 hour to achieve better crystallization.

2.2. Characterization techniques

Several characterization methods were used to investigate the effect of substrate type on the physical properties of the RF sputter deposited TiO_2 thin films. The identification of crystalline nature and phases was performed on Rigaku MiniFlex II diffractometer using Cu*K*α X-rays (λ = 0.15406 nm). The samples were scanned from 20° to 55° with a step size of 0.017° (2θ). Raman scattering spectra were carried out at room temperature using a HORIBA/Jobin-Yvon LabRam micro-Raman apparatus (HR-800). The monochromatic irradiation source is an argon ion laser with a wavelength of 514 nm. This radiation was focused on the surface of the sample using an Olympus confocal microscope equipped with a × 100 objective. The spectra were recorded in the range 80-1000 cm^{-1} and the accumulation time was been adjusted to obtain the best signal to noise ratio. The surface morphology of the samples was inspected by SEM on a Raith PIONEER system. The topography and surface roughness of the films were evaluated by AFM. The experiments were performed in contact mode by a Nanosurf Flex-AFM system equipped with a 10 µm × 10 µm high resolution scanner. AFM images were recorded with a resolution of 256 × 256 pixels over scanning areas of 2×2 μm^2, and the Gwyddion software was used for image processing and surface roughness calculations [49]. A Safas UVmc^2 ultraviolet–visible (UV–Vis) spectrophotometer was used to measure the optical transmittance spectra in the range of 250-1050 nm. The optical bandgap energy was then derived from the transmittance data. A Veeco Dektak 150 Surface Profiler was used to measure film thickness. The thickness of the TiO_2 films is found to be 150 ± 2 nm.

3. Results and discussion

3.1. XRD analysis

Figure 1 shows the XRD patterns of TiO_2 thin films deposited on three different substrates (glass, amorphous quartz and SiO_2/Si). It can be noticed that all TiO_2 thin films are found to be polycrystalline having an anatase structure (TiO_2, JCPDS card # 04-0477) with preferred orientation along the (101) direction. Diffraction peaks belonging to anatase (004), (200) and (105) planes are also detected. However, no characteristic peaks of brookite and/or rutile appeared in the XRD spectra for all samples. It can clearly be seen that the peaks intensity was changed, indicating the effect of substrate type on the crystalline properties. The TiO_2 thin film deposited on crystalline Si substrate shows the best crystallinity as compared to those prepared on amorphous quartz and glass substrates. This

may be attributed to the fact that the crystalline Si(100) with long-range ordered structure provides more fixed lattices for reactive atoms or clusters to land and solidify than the long-range disordered amorphous quartz and glass structures [50].

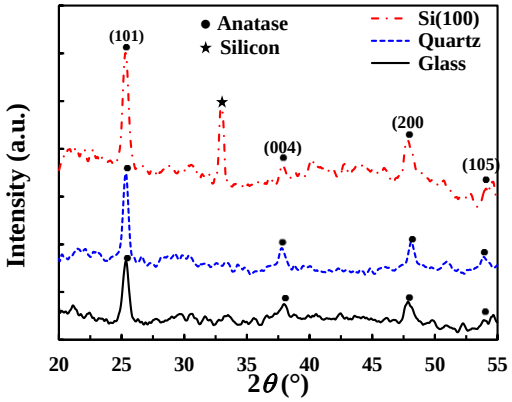

Figure 1. XRD patterns of TiO_2 thin films grown on glass, quartz and Si(100) substrates.

In order to investigate the influence of substrate types on the crystallite growth, the average crystallite size of the samples was estimated from the full-width at half-maximum (FWHM) of the most intense peak of anatase structure corresponding to (101) reflection with the help of the Scherrer equation [51]:

$$D = \frac{0.9\lambda}{\beta \sin\theta} \quad (1)$$

where D is the average crystallite size in nanometers, λ is the wavelength of the incident Cu Kα radiation (0.154056 nm), θ is the Bragg angle and β is the FWHM of the XRD signal with peak position at θ.

Figure 2 illustrates the variations of the average crystallite size and FWHM of TiO_2 thin films as a function of substrate types.

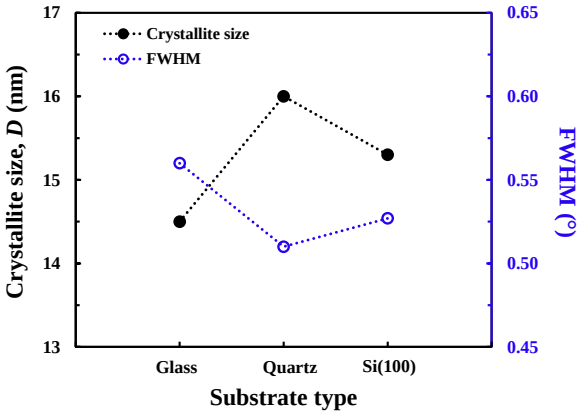

Figure 2. Crystallite size and FWHM of TiO_2 thin films grown at different types of substrates.

As can be seen, the FWHM decreases from 0.56° to 0.51° an then increases to 0.53° for the TiO_2 films deposited on glass, quartz and Si(100) substrates. The calculated average crystallite size is found to be about 14.5, 16.0 and 15.3 nm, respectively. These observations suggest that the structural property of the TiO_2 thin films is strongly influenced by the type of the substrate, which in consistent with results obtained in a previous study [52]. This may be attributed to the fact that the mobility of the atoms on the surface of the substrate, which is responsible for the degree and type of nucleation on the substrate.

3.2. Raman spectroscopy study

The Visible Raman spectroscopy was also carried out to investigate both microstructure and crystalline quality of the prepared TiO_2 thin films. Figure 3 shows Raman spectra of the TiO_2 thin films deposited on different types of substrates in the range of 100-800 cm^{-1}.

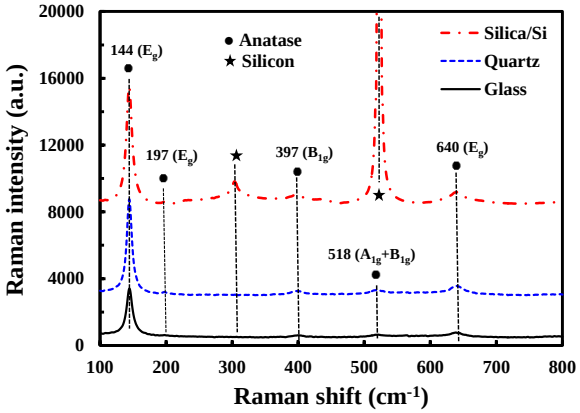

Figure 3. Raman spectra of TiO_2 thin films grown on glass, quartz and Si(100) substrates.

It can be seen that crystallization and anatase structures appear in all samples regardless the substrate type. The observed band positions are in good agreement with those reported in previous works for anatase phase [53, 54]. The Raman modes at 144, 197, 397, 518 and 640 cm^{-1} are assigned to the E_g, E_g, B_{1g}, A_{1g} and E_g modes, respectively, in the anatase phase structure [55]. The presence of a strong peak located at 144 cm^{-1} arising from the external vibration of the anatase structure is well pronounced; indicating that the anatase phase with a long-range order is present in all TiO_2 films. The Raman peaks of TiO_2 film grown on Si(100) substrate show higher intensities compared to those deposited on quartz and glass substrates suggesting that the crystalline quality of the prepared films is affected by the substrate type, which is in complete agreement with the above XRD results. It should be noted that the Raman peak of the TiO_2 thin film grown on Si(100) measured around 303 cm^{-1} is ascribed to the

overtone of 2TA(X) of the silicon substrate. Moreover, due to the high penetration depth of the 514 nm laser line, the very strong peak at 522.5 cm^{-1} from the LO phonon line of silicon is visible in the Raman spectrum, which masks the 518 cm^{-1} line from the anatase phase [56].

Figure 4 displays the main anatase mode peak located at 144 cm^{-1} as a function of the substrate type. It can clearly be seen that the FWHM of the band was altered, indicating the impact of the substrate type. The FWHM decreased from 10.0 cm^{-1} to 9.1 cm^{-1} then increased to 11.6 cm^{-1} for the TiO_2 films deposited on glass, quartz and Si(100) substrates, respectively, suggesting a changes in crystallite size in good agreement with the above XRD data.

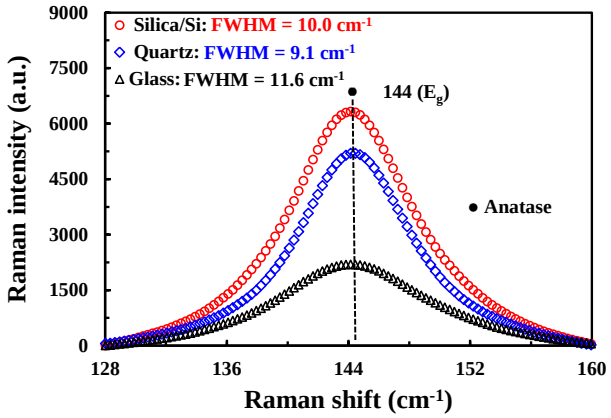

Figure 4. Enlarged view of the E_g mode (144 cm^{-1}) spectra of TiO_2 thin films grown on glass, quartz and Si(100) substrates.

3.3. Surface morphology and topography

Figure 5 shows top-view SEM micrographs taken at 50,000x magnifications of TiO_2 thin films prepared under the same conditions on glass, quartz and Si(100) substrates. As can be seen, the surface structures of TiO_2 thin films are different, putting clearly into evidence the effects of the substrate type. In fact, The TiO_2 film grown on glass substrates is found to exhibit a smooth surface that consists of a very small spherical like grains with almost uniform size and aggregates of such particles, along with some pores distributed over the film surface. Whereas TiO_2 film deposited on quartz substrates shows a very smooth surface with a more uniform and compact distribution of the grains. An increase in the grain size is also observed, indicating an enhancement in the crystallinity. However, the TiO_2 film prepared on the Si(100) substrate shows significantly different surface features characterized by the formation of smaller size grains than those on quartz and larger than those on glass substrate distributed homogenously over the surface. The latter behavior in the grain morphology may be attributed to the crystallite growth of the film on the crystalline nature of the Si(100) substrate. Moreover, it can be concluded that grain size depends on the substrate nature and shows similar trend to that of crystallite size revealed by XRD data.

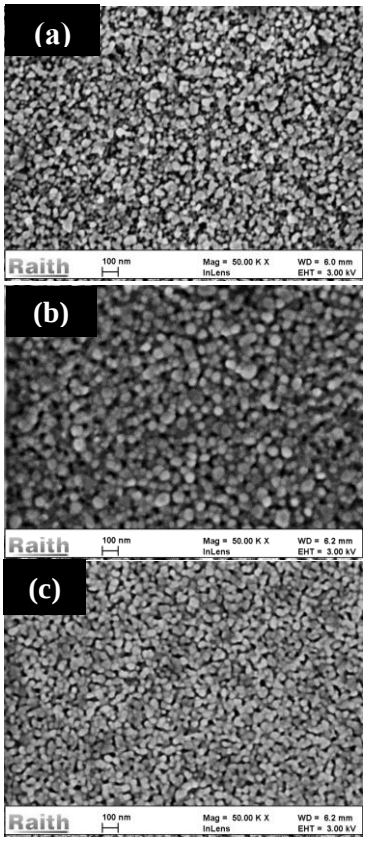

Figure 5. Top-view SEM images of TiO_2 thin films grown at different types of substrates: (a) glass, (b) quartz, and (c) Si(100).

TiO_2 thin films were further analyzed by AFM technique in the contact mode to investigate their topography and surface roughness. Figure 6 illustrates the two-dimensional (2D) and three-dimensional (3D) AFM topography images of TiO_2 thin films prepared under the same conditions on glass, quartz and Si(100) substrates recorded over a 2.0 µm × 2.0 µm scanning area. It can be seen that TiO_2 thin films exhibit a different surface topography with the agglomerates growing up along the surface, which seems to be strongly affected by the substrate type. From data analysis, one can deduce root mean square roughness (R_{rms}) values of 5.91, 4.12 and 8.80 nm for TiO_2 thin films grown on glass, quartz and Si(100) substrates, respectively. The TiO_2 film prepared on Si(100) substrate possess a larger surface roughness, which is higher than the films grown on glass and quartz) substrates. The present results are consistent with those obtained by Cheng *et al.* [26]. They have reported that

TiO_2 thin film deposited by DC sputtering method on Si(111) substrate is much rougher than films deposited on glass substrate, which was related to the higher density of anatase nuclei forming on crystalline surface during deposition. It should be noted that the TiO_2 sample prepared on quartz substrate shows the smallest surface roughness value.

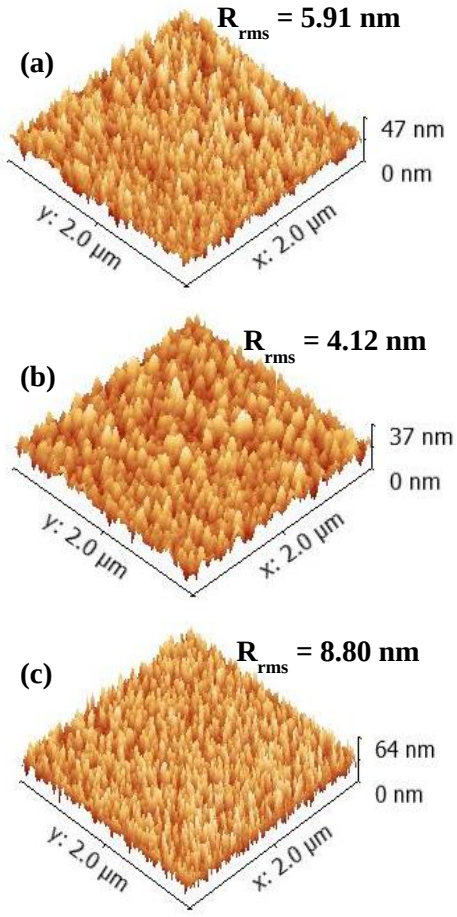

Figure 6. 3D AFM images of TiO_2 thin films grown at different types of substrates: (a) glass, (b) quartz, and (c) Si(100).

3.4. Optical properties

The optical transmittance is an essential parameter in determining the quality of transparent conducting oxides. It should be noted that since silicon is an opaque substrate, we will see almost nothing in transmittance below roughly 1000 nm and transmittance spectra can be measured only for the transparent substrates. Thus, TiO_2 thin films prepared on transparent substrates were studied at room temperature in the 200–1050 nm wavelength range in order to obtain optical constants such as transmission (T) and optical band gap energy (E_g). Figure 7 illustrates the optical transmittance spectra of the TiO_2 thin films grown on glass and quartz substrates and measured with respect to substrate. The data demonstrate a high transmission in the visible spectral region (400 - 800 nm). The average transmittance on glass substrate is about 81.94% and increases to about 83.64% for quartz substrate. The increase in average transmittance may be attributed to the morphological changes, structure with enhanced crystalline quality, as well as lower surface roughness as revealed by XRD data and AFM images.

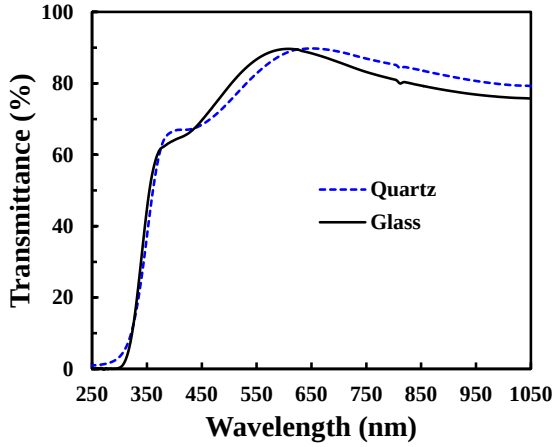

Figure 7. Optical transmittance spectra of TiO_2 thin films grown on glass and quartz substrates.

Optical band gap of semiconductor thin films is of great importance in several potential fields, in particular photovoltaic and optoelectronic applications To investigate the effect of substrate type on the direct optical band gap (E_g) of TiO_2 thin films, we use the method based on the first derivative of transmittance (T) as a function of photon energy (E) whose detailed description can be found elsewhere [57]. The importance of such technique lies in its applicability to the determination of an accurate energy gap band value without knowing the film thickness. Based on the measured transmittance spectra, the dT/dE curves of the TiO_2 samples deposited on glass and quartz substrates are displayed in Figure 8. Band gap values of 3.615 and 3.512 eV are obtained for the samples grown on glass and quartz substrates, respectively. These values show a good agreement with previous reported direct optical band gap values of TiO_2 thin films ranging from 3.50 to 3.80 eV [58, 59]. The decrease in the band gap energy of the TiO_2 film deposited on quartz substrate may be attributed to the improvement of crystallinity of anatase phase along with morphological changes. Indeed, it has been reported that red-shift of band gap in thin films may be attributed to different reasons such as enhancement in crystallinity, variation in crystallite dimension, increase of the grain size and quantum size effect [60, 61].

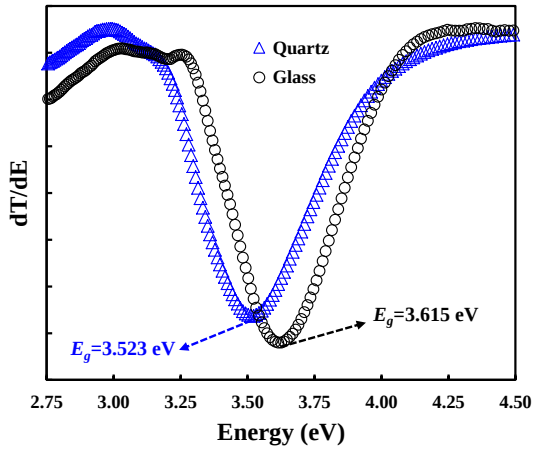

Figure 8. d*T*/d*E* curves based on transmittance spectra of TiO_2 thin films grown on glass and quartz substrates.

Refractive index (*n*) of semiconductor thin films is an essential parameter to be determined in order to be used in the design and fabrication of desired optical elements and devices To do so, we adopted the methodology applied by Duffy [62, 63] to a number of simple oxides such as SiO_2, MgO and TiO_2. In fact, Duffy [62] proposed the following relation between the linear refractive index and the optical band gap:

$$E_g = 20\left(1 - \frac{n^2+1}{n^2+2}\right)^2 \quad (2)$$

We used this equation, applicable to various oxides [64], to estimate the refractive index of TiO_2 thin films from the energy gap. Form Eq. (2) we deduce the following explicit expression of *n*:

$$n = \left(\frac{3-2\sqrt{E_g/20}}{\sqrt{E_g/20}}\right)^{\frac{1}{2}} \quad (3)$$

The obtained data showed that the linear refractive index of the films is found to be 2.248 and 2.271 for TiO_2 films deposited on glass and quartz substrates, respectively.. The refractive index enhancement may be ascribed to the increase in packing density owing to the further particle agglomeration during deposition and after annealing. Moreover, this tendency for the refractive index to increase in the case of quartz substrate is in good agreement with the improvement in crystallinity and better densification of the TiO_2 films as revealed by XRD spectra and SEM images.

4. Conclusion

TiO_2 thin films have successfully been deposited on glass substrates by the RF magnetron sputtering technique. The dependencies of the structural, morphological and optical properties on the annealing temperature (350, 450 and 550°C) have been systematically investigated. XRD spectra have shown that all the TiO_2 thin films are polycrystalline having anatase phase only with a preferential orientation of (101). Moreover, increasing annealing temperature has been found to improve the crystallinity and crystallite growth. The Raman studies have confirmed that TiO_2 films have crystallized in the tetragonal anatase phase and their crystal quality has been enhanced with annealing. SEM and AFM images have revealed that the as-deposited film demonstrated homogeneous and smooth surface consisting of small grain size particles, whereas increasing the annealing temperature resulted in more compact film with larger grain size and rougher surfaces. The UV–Vis. measurements have shown that the as-deposited TiO_2 film is highly transparent with an average transmittance of 84 % in the visible region. With increasing annealing temperature a decrease in the average transmittance and a red shift in the direct optical band gap from 3.76 to 3.50 eV have been observed.

References

[1] H. Wang, R. Zhang, Z. Yuan, X. Shu, E. Liu, Z. Han, Ceram. Int. 41 (2015) 1844.
[2] Y. Zhang, S. Zhang, S. Wu, Chem. Eng. J. 371 (2019) 609.
[3] K. Nakata, A. Fujishima, J. Photochem. Photobiol. C 13 (2012) 169.
[4] B. Lyson-Sypien, A. Czapla, M. Lubecka, Sens. Actuat. B: Chem. 187 (2013) 445.
[5] R.P. Cavalcante, R.F. Dantas, B. Bayarri, O. González, J. Giménez, S. Esplugas, A.M. Junior, Appl. Catal. B-Environ. 194 (2016) 111.
[6] M.I. Khana, K.A. Bhatti, R. Qindeel, H.S. Althobaiti, and N. Alonizan , Results. Phys. 7 (2017) 143.
[7] M. Atoui, T. Touam, I. Hadjoub, A. Chelouche, B. Boudine, A. Fischer A. Boudrioua, A. Doghmane, Int. J. Nanotechnology 12 (2015) 572.
[8] Q. Wang, K. Zhu, N.R. Neale, A.J. Frank, Nano. Lett. 9 (2009) 806.
[9] C. Dette, M. Perez-Osorio, C.S. Kley, P. Punke, C.E. Patrick, P. Jacobson, F. Giustino, S.J. Jung, K. Kern, Nano Lett. 14 (2014) 6533.
[10] H. Saleem, A. Habib, J. Alloys Compd. 679 (2016) 177.

[11] H. Tang, F. Lévy, H. Berger, P.E. Schmid, Phys. Rev. B Condens. Matter 52 (1995) 7771.
[12] J.X. Liu, D.Z. Yang, F. Shi, Y.J. Cai, Thin Solid Films 429 (2003) 225.
[13] C.H. Lee, K.H. Kim, H.W. Choi, Mol. Cryst. Liq. Cryst. 567 (2012) 9.
[14] S. Zaitsu, T. Jitsuno, M. Nakatsuka, T. Yamanak, S. Motokoshi, Appl. Phys. Lett. 80 (2002) 2442.
[15] H.C. Barshilia, K.S. Rajam, J. Mater. Res. 19 (2004) 3196.
[16] J. Criado, C. Real, J. Chem. Soc., Faraday Trans. 179 (1983) 2765.
[17] M.W. Pyun, E.J. Kim, D.H.Yoo, S.H. Hahn, Appl. Surf. Sci. 257 (2010) 1149.
[18] . M. Alotaibi, S. Sathasivam, B.A.D. Williamson, A. Kafizas, C.S.Vazquez, A. Taylor, D.O. Scanlon, I.P. Parkin, Chem. Mater. 30 (2018) 1353.
[19] O. Chibani, F. Challali, T. Touam, A. Chelouche, D. Djouadi, Opt. Eng. 58 047101 (2019) 047101.
[20] A. Juma, I.O. Acik, A.T. Oluwabi, A. Mere, V. Mikli, M. Danilson, M. Krunks, Appl. Surf. Sci. 387 (2016) 539.
[21] T.D. Dongale, S.S. Shinde, R.K. Kamat, K.Y. Rajpure, J. Alloys. Compd. 593 (2014) 267.
[22] N. Méndez-Lozanoa, M. Apátiga-Castro, A. Manzano-Ramírez, E.M. Rivera-Muñoz, R. Velázquez-Castillo, C. Alberto-González, M. Zamora-Antuñano, Results Phys. 16 (2020) 102891.
[23] L. Meng, Z. Wang, L. Yang, W. Ren , W. Liu, Z. Zhang, T. Yang, M.P. dos Santos, Appl. Surf. Sci. 474 (2019) 211.
[24] C. Yang, H.Q. Fan, Y.X. Xi , J. Chen, Z. Li, Appl. Surf. Sci. 254 (2008) 2685.
[25] H. Nagasawa, J. Xu M. Kanezashi, T. Tsuru, Mater. Lett. 228 (2018) 479.
[26] C.C. Tsai, Y.Y. Chu, H. Teng, Thin Solid Films 519 (2010) 662.
[27] J.E. Hu, S.Y. Yang, J.C. Chou, P.H. Shih, Micro Nano Lett. 7 (2012) 1162.
[28] C.H. Heo, S. B. Lee, J.H. Boo, Thin Solid Films 475 (2005) 183.
[29] I. Turkevych, Y. Pihosh, M. Goto, A. Kasahara, M. Tosa, S. Kato, K. Takehana, T. Takamasu, G. Kido, N. Koguchi, Thin Solid Films 516 (2008) 2387.
[30] H.E. Doghmane, T. Touam, A. Chelouche, F. Challali, B. Bordji, Semiconductors 54 (2020) 268.
[31] S.M. Chiu, Z.S. Chen, K.Y. Yang, Y.L. Hsu , D. Gan, J. Mater. Process. Technol. 192–193 (2007) 60.
[32] B. Astinchap, R. Moradian, K. Gholami, Mater. Sci. Semicond. Process. 63 (2017) 169.
[33] M.M. Hasan, A.S.M.A. Haseeb, R. Saidur, H.H. Masjuki, M. Hamdi, Opt. Mater. 32 (2010) 690.
[34] F. Meng, Z. Sun, Mater. Chem. Phys. 118 (2009) 349.
[35] T.M. Wang, S.K. Zheng, W.C. Hao, C. Wang, Surf. Coat. Technol. 155 (2002) 141.
[36] A.R.G. Korpi, S. Rezaee, C. Luna, Ş. Ţălu, A. Arman, A.A. Pourian, Results Phys. 7 (2017) 3349.
[37] N. Kawashima, Q.Y. Zhu, A.R. Gerson, Thin Solid Films 520 (2012) 3884.
[38] R. Shakoury, A. Zarei, Silicon 11 (2019) 1247.
[39] F. Meng, F. Lu, Vacuum 85 (2010) 84.
[40] M. Sreedhar, I.N. Reddy, Appl. Phys. A 120 (2015) 765.
[41] A. Majeed, J. He, L.i Jiao, X. Zhong, Z. Sheng, Nanoscale Res. Lett. 10 (2015) 56.
[42] A.H. Haseeb, M.M. Hasan, H.H. Masjuki, Surf. Coat. Technol. 205 (2010) 338.
[43] X. Zhu, P. Gu , H. Wu, D. Yang, H. Sun, P. Wangyang, J. Li, H. Tian, AIP Adv. 7 (2017) 2158.
[44] S. Nezar, N. Saoula, S. Sali, M .Faizd, M. Mekki, N.A. Laoufi, N. Tabet, Appl. Surf. Sci. 395 (2017) 172.
[45] Y.H. Wang, K.H. Rahman, C.C. Wu, K.C. Chen, Catalysts 10 (2020) 598.
[46] F. Meng, L. Xiao, Z. Sun, J. Alloys Compd. 485 (2009) 848.
[47] P.B. Nair, V.B. Justinvictor, G. P. Daniel, K. Joy, V. Ramakrishnan, P.V. Thomas, Appl. Surf. Sci. 257 (2011) 10869.
[48] H. Sun, C. Wang, S. Pang, X. Li, Y. Tao, H. Tang, M .Liu, J. Non-Cryst. Solids 354 (2008) 1440.
[49] D. Nečas, P. Klapetek, Cent. Eur. J. Phys. 10 (2012) 181.
[50] X. Cheng, K. Gotoh, Y. Nakagawa, N. Usami, J. Cryst. Growth 491 (2018) 120.
[51] J.I. Langford, A.J.C. Wilson, J. Appl. Cryst. 11 (1978) 102.
[52] C.-H. Wei, C.-M. Chang, Mater. Trans. 52 (2011) 554.
[53] F. Rossella, P. Galinetto, M.C. Mozzati, L. Malavasi, Y. Diaz Fernandez, G. Drera, L. Sangaletti, J. Raman Spectrosc. 41 (2010) 558.
[54] O. Chibani, T. Touam, A. Chelouche, L. Ouarez, J. Alloys Compd. 768 (2018) 866.
[55] T. Ohsaka, F. Izumi, Y. Fujiki, J. Raman Spectrosc. 7 (1978) 321.
[56] X. Wang, J. Shen, Q. Pan, J. Raman Spectrosc. 42 (2011) 1578.
[57] T. Touam, M. Atoui, I. Hadjoub, A. Chelouche, B. Boudine, A. Fischer, A. Boudrioua, A. Doghmane, Eur. Phys. J. Appl. Phys. 67 (2014) 30302.
[58] M.H. Habibi, N. Talebian, J.H. Choi, Dyes Pigments 73 (2007) 103.
[59] C. Yang, H. Fan, Y. Xi, J. Chen, Z. Li, Appl. Surf. Sci. 254 (2008) 2685.

[60] M. Suchea, S. Christoulakis, M. Katharakis, N. Vidakis, E. Koudoumas, Thin Solid Films 517 (2009) 4303.
[61] X. Wang, G. Wu, B. Zhou, J. Shen, Mater. 6 (2013) 2819.
[62] J. A. Duffy, Solid State Chem. 62 (1986) 145.
[63] J. A. Duffy, J. Am. Ceram. Soc. 72 (1989) 2012.
[64] V. Dimitrov, S. Sakka, J. Appl. Phys. 79 (1996) 1736.